I&EC research
Industrial & Engineering Chemistry Research

Article

pubs.acs.org/IECR

Solid State Foaming of Poly(lactic acid) Blown with Compressed CO_2: Influences of Long Chain Branching and Induced Crystallization on Foam Expansion and Cell Morphology

Qian Ren,[†,‡] Jingjing Wang,[†,§] Wentao Zhai,[†,*] and Shengpei Su[‡]

[†]Ningbo Key Lab of Polymer Materials, Ningbo Institute of Material Technology and Engineering, Chinese Academy of Sciences, Ningbo, Zhejiang Province 315201, China

[‡]College Chemistry & Chemical Engineering, Hunan Normal University, Changsha 410081, Hunan, China

[§]The School of Materials Science and Chemical Engineering, Ningbo University, Ningbo, Zhejiang Province 315211, China

ABSTRACT: In this study, poly(lactic acid) (PLA) resins with linear (L-PLA) and branched structure (B-PLA) were selected, and the solid state foaming technology was applied to prepare PLA foams. B-PLA foams exhibited a high expansion ratio of about 40 and cell density of 10^{5-6} cells/cm^3, whereas L-PLA foams only had the highest expansion ratio of 29.8 and cell density of 10^{3-6} cells/cm^3. When PLA resins were induced crystallization during CO_2 saturation, however, the prepared L-PLA foams presented the highest expansion ratio of 37.4 and cell density of 10^{6-7} cells/cm^3. The cell structure evolution of PLA foams with the foaming time suggested that the in situ formed crystal domains supplied nucleating sites to enhance cell nucleation and acted as physical cross-linking points to stabilize cell structure. These interesting results demonstrated that the induced crystallization might be more attractive than the chain modification to improve the foaming behavior using solid state foaming technology.

■ INTRODUCTION

With the global need to protect the natural environment and conserve petroleum resources, biobased plastics obtained from renewable resources continue to garner much attention.[1,2] Poly(lactic acid) (PLA) is a shining star among the biobased plastics owing to its high modulus, high strength, and excellent transparency.[1−3] However, PLA suffers from a low crystallization rate, low glass transition temperature, and high cost, which limits its application in the packaging industry.[3] To compensate for the shortcomings of PLA, researchers from academic and industrial fields have commited to foaming technology. A good reason is that foaming contributes to the development of crystallinity,[4−7] which potentially improves the thermal stability of PLA and reduces the sample usage.

Extrusion foaming and injection molding foaming with high efficiency are popular approaches to fabricate polymeric foams.[5,8−16] Unfortunately, PLA usually presents poor foaming behavior and a very narrow foaming window due to its low melt strength.[16] To address this issue, researchers synthesize high melt strength PLA using a chain extender[11−13,16,17] or compounding with nanofillers.[18,19] The chain modifications do improve the foaming behavior of PLA, and the prepared PLA foams exhibit a well-defined cell morphology, higher expansion ratio, and broader foaming temperature window.[16] In the case of injection molding foaming, the chain modifications are beneficial for the generation of a uniform and tine cell structure.[14] Recently, Nature Works LLC has commercialized several kinds of high melt strength PLA resin grades for foaming. Park's group carried out extrusion foaming research based on the PLA resins. The study proved that PLA with linear structure (L-PLA) had a foam expansion of 3−5, while the foam expansion of PLA with long chain branching (B-PLA) was as high as 30−40. Furthermore, the cell density of B-PLA foams was about 10^{7-9} cells/cm^3.[16] However, there is cost challenge to wide use, as the B-PLA resin costs at least twice as much as the L-PLA.

Solid state foaming is another approach to prepare PLA foams,[6,7,19−25] where the compressed CO_2 is usually used as the physical blowing agent. PLA presents low crystallization rate at the atmospheric pressure (AP). Under high CO_2 pressure, however, the strong plasticization effect of compressed CO_2 increases the crystallization rate of PLA significantly,[26,27] which leads to the crystallinity development.[4] The formed crystal domains cannot absorb gas, and it works as inert solid to enhance heterogeneous cell nucleation.[28,29] At the same time, the crystal domains can work as cross-linking points to increase the melt strength of polymer, which potentially affects the cell growth.[30] Therefore, in solid state foaming process, it is possible to adjust the foaming behavior of PLA by controlling the induced crystallinity and crystal size.[23] Similar adjustment of cell morphology had been observed at other foaming systems such as polypropylene (PP)/CO_2, where the regular PP resins were foamed in solid states.[31−33] This means that high melt strength PLA may not be necessary in the preparation of desirable PLA foam with a high expansion ratio and well-defined cell structure using solid state foaming technology.

In this study, two PLA resins, i.e., L-PLA and B-PLA, with similar D content were selected to fabricate PLA foams using solid state foaming technology, where B-PLA was obtained by chain extension of L-PLA. Compressed CO_2 was used as the blowing agent. The crystallinity of the gas saturated PLA resins

Received: June 28, 2013
Revised: August 11, 2013
Accepted: August 16, 2013
Published: August 16, 2013

ACS Publications dx.doi.org/10.1021/ie402039y | *Ind. Eng. Chem. Res.* 2013, 52, 13411−13421

were controlled by the pressure of CO_2. The foaming behavior of L-PLA and B-PLA at various foaming temperatures and times were investigated to show the effects of long chain branching and induced crystallization on the expansion ratio and cell morphology of PLA foams. The effect of crystal size on the cell nucleation behavior of PLA was also addressed.

■ EXPERIMENTAL SECTION

Materials and Sample Preparation. Two types of semicrystalline PLA with linear (8051D) and long chain branched structures were supplied by Nature Works LLC in two formulations with similar D-lactide molar content (4.5−4.6 mol %). B-PLA was produced by reactive extrusion with an epoxy-based multifunctional oligomeric chain extender (Joncryl ADR-4368C, BASF Inc.) based on L-PLA with 0.7 wt % of CE. The molecular weights of L-PLA and B-PLA were 90 000 and 113 000 g/mol, respectively.[16,26] CO_2 with a purity of 99.9% obtained from Ningbo Wanli Gas Corporation was used as the physical blowing agent in all experiments. The PLA pellets were oven-dried at 70 °C for at least 10 h before use. Samples with a thickness of 0.5 mm were prepared by compression molding at 200 °C and then quenched to room temperature by cold water. The sheets were cut into specimens of 15 mm × 15 mm for foaming experiments.

Batch Foaming. The PLA specimens were enclosed in a high-pressure vessel at room temperature. The vessel was flushed with low pressure CO_2 for about 1 min, followed by increasing the pressure and then pressurized to the desired value. The samples were saturated under this condition for 12 h to ensure equilibrium adsorption of CO_2. At the end of the experiment, the vessel was released with a depressurization rate of 10 MPa/s, and then the specimens were transferred within 1 min to the water bath with the fixed temperature. The samples were foamed in the water or oil bath for 20 s unless indicated and then quenched in cold water with the temperature of 15 °C. The oil bath was used when the foaming temperatures were higher than 100 °C.

Characterization. An atomic force microscope (AFM, CSPM5500, Benyuan, China) in trapping mode was used to observe the actual crystal morphology of the gas-saturated PLA samples. The PLA/chloroform solution with a concentration of 0.1 wt % was prepared by magnetic stirring for 3 h. About 30 μL of the PLA solution was simply deposited on freshly cleaved mica. The samples were then allowed to evaporate under ambient conditions (25 °C and 55% of relative humidity) in a Petri dish for at least 20 min before use.

The melting behavior of PLA samples was determined using an apparatus (Mettler Toledo DSC/TGA) calibrated with indium. For all CO_2 saturated samples, a long gas desorption time, e.g., at least one month, under AT and room temperature was carried out to avoid the possible effect of gas plasticization on sample's crystallinity. All measurements were carried out with a heating rate of 10 °C/min over a temperature range from 25 to 200 °C in a dry nitrogen environment. The degree of crystallinity was calculated by $[(\Delta H_m - \Delta H_c)/\Delta H_f] \times 100\%$, where ΔH_m and ΔH_c are the heat of fusion generated by the crystals melting and cold crystallization and ΔH_f is the theoretical heat of fusion of 100% crystalline PLA with a value of 93 J/g.[34]

The mass densities of the samples before (ρ) and after (ρ_f) foaming were measured via water displacement method according to ISO 1183−1987. The uptake of water by the samples can be neglected during this measurement due to a smooth skin and closed cells of these foamed samples.

The cell structures were investigated by using a Hitachi TM-1000 scanning electron microscope (SEM). The samples were freeze-fractured in liquid nitrogen and sputter-coated with gold. The cell size and cell density were obtained through the SEM photographs. The cell density (N_0), the number of cells per cubic centimeter of solid polymer, was determined using eq 1 as follows:

$$N_0 = \left[\frac{nM^2}{A}\right]^{3/2}\phi \qquad (1)$$

where n is the number of cells in the SEM micrograph, M is the magnification factor, A is the area of the micrograph (in cm^2), and ϕ is the volume expansion ratio of the polymer foam, which can be calculated using eq 2 as follows:

$$\phi = \frac{\rho}{\rho_f} \qquad (2)$$

where ρ and ρ_f are the densities of PLA resin and PLA foam.

■ RESULTS AND DISCUSSION

Rheological and Crystallization Behaviors of L-PLA and B-PLA. In general, the cell growth process is an extensional flow of the polymer/gas solution in nature.[35] The factors that affect the viscoelastic properties of a polymer melt usually affect its foaming behavior. In our previous study, Wang et al. investigated the extensional viscosity of the L-PLA and B-PLA, and the strain rates of 0.1−3.0 s^{-1} were applied.[16] They found that L-PLA exhibited little strain hardening and necking of the sample. In contrast, the extensional viscosities of B-PLA were significantly strain hardening at all extensional rates. In the extrusion foaming, they verified that the increased extensional viscosity improved the foaming behavior of PLA.

The induced crystallization of semicrystalline polymers after CO_2 saturation affects the foaming behavior.[23,25,28,36,37] Figure 1 shows the DSC thermograms of L-PLA and B-PLA at AP and various CO_2 pressures. At AP, both L-PLA and B-PLA had a broad cold crystallization peak at around 124 °C and a melting peak at around 150 °C. After CO_2 saturation at 2.5 MPa, L-PLA and B-PLA presented a sharp cold crystallization peak at the temperature of 114 °C and a melting temperature at around 150 °C. A further increase in CO_2 pressure to 3.5 MPa tended

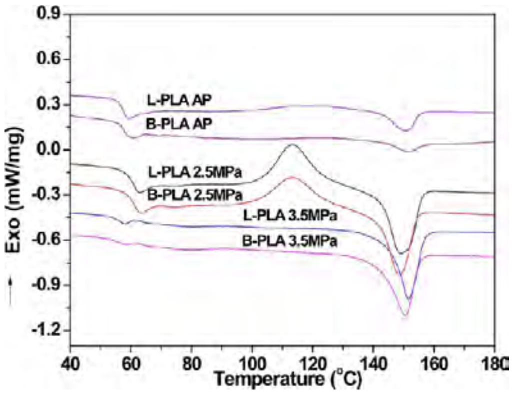

Figure 1. DSC curves of PLA samples saturated at AP and various CO_2 pressures.

to obviously affect the crystallization behavior of PLA samples, where no detectable cold crystallization was observed.

Table 1 summarizes the crystallinity of the CO_2 saturated and foamed PLA samples. Both L-PLA and B-PLA samples were amorphous after compression molding. After the CO_2 saturation treatment at 2.5 MPa, L-PLA and B-PLA presented very slight crystallization with crystallinities of about 2.1% for L-PLA and 1.3% for B-PLA, respectively. Considering the inevitable calculation error of the integration of cold crystallization peak and melting peak, in this study, we treated the saturated PLA samples at 2.5 MPa as amorphous, and the obtained PLA samples were coded as AL-PLA and AB-PLA. With increasing the saturation pressure to 3.5 MPa, however, PLA samples were induced to crystallize and then were coded as CL-PLA and CB-PLA. The crystallinity was 25.0% for CL-PLA and 23.2% for CB-PLA.

Table 1. Crystallinity of the CO_2 Saturated and Foamed PLA Samples

samples	saturation pressure MPa	crystallinity (%)
L-PLA	AP	0
B-PLA	AP	0
L-PLA	2.5	~2.1
B-PLA	2.5	~1.3
L-PLA	3.5	25.0
B-PLA	3.5	23.2
samples	**foaming conditions**	**crystallinity (%)**
L-PLA foam	2.5 MPa/80 °C	16.7
B-PLA foam	2.5 MPa/80 °C	17.2
L-PLA foam	3.5 MPa/80 °C	33.5
B-PLA foam	3.5 MPa/80 °C	32.9

Usually, the semicrystalline PLA exhibits a low crystallization rate. Under compressed CO_2, however, the strong plasticization effect of CO_2 increases the mobility of the polymer chain and hence allows the fast relaxation of polymer chains,[38,39] resulting in an increased crystallization rate.[26,40] By using high pressure DSC, Nofar et al. measured the glass transition temperature (T_g) of the L-PLA and B-PLA at various CO_2 pressures.[26] They found that the T_g of the PLA sample at AP was about 55 °C, and the CO_2 saturation treatment linearly decreased the plasticized T_g of PLA to 42 °C at 1.5 MPa, 31 °C at 3.0 MPa, 26 °C at 4.5 MPa, and 18 °C at 6.0 MPa, respectively, with the DSC cooling rate of 2 °C/min.[26] In our study, the saturation temperature was about 25 °C, the compressed CO_2 at 2.5 MPa did not induce the obvious crystallization of PLA, while at 3.5 MPa the formation of high crystallinity was observed. This was in accord with the high pressure DSC data, which proved that the decreased T_g was the main reason for the induced crystallization of PLA. Besides the gas saturation process, the foaming process at high temperature is also beneficial for the crystallization development. It is seen from Table 1 that the crystallinity of foamed L-PLA and B-PLA was 16.7% and 17.2% at 2.5 MPa and was 33.5% and 32.9% at 3.5 MPa, respectively. Similar crystallinity development had been observed in the PLA foaming process.[4,8,25] This was possibly attributed to the high temperature treatment and volume expansion of the saturated samples during the foaming.[4,8]

AFM topography images were used to show the surface morphology of the CO_2 saturated PLA samples, and the results are shown in Figure 2. The untreated L-PLA and B-PLA samples were amorphous, and the surface morphologies were possibly induced by the evaporation of solvent during the sample preparation. After CO_2 treatment at 2.5 MPa, however, the surface morphologies of PLA changed obviously, which indicated that the compressed CO_2 increased the mobility of polymer chains and induced the occurrence of chains rearrangement. At 3.5 MPa, the obvious spherulite structures could be seen in the saturated L-PLA, while the formed crystal structure of the saturated B-PLA was rod. Furthermore, the CO_2 saturation at 3.5 MPa endowed B-PLA with much smaller crystal size and much higher crystal density compared to the saturated L-PLA.

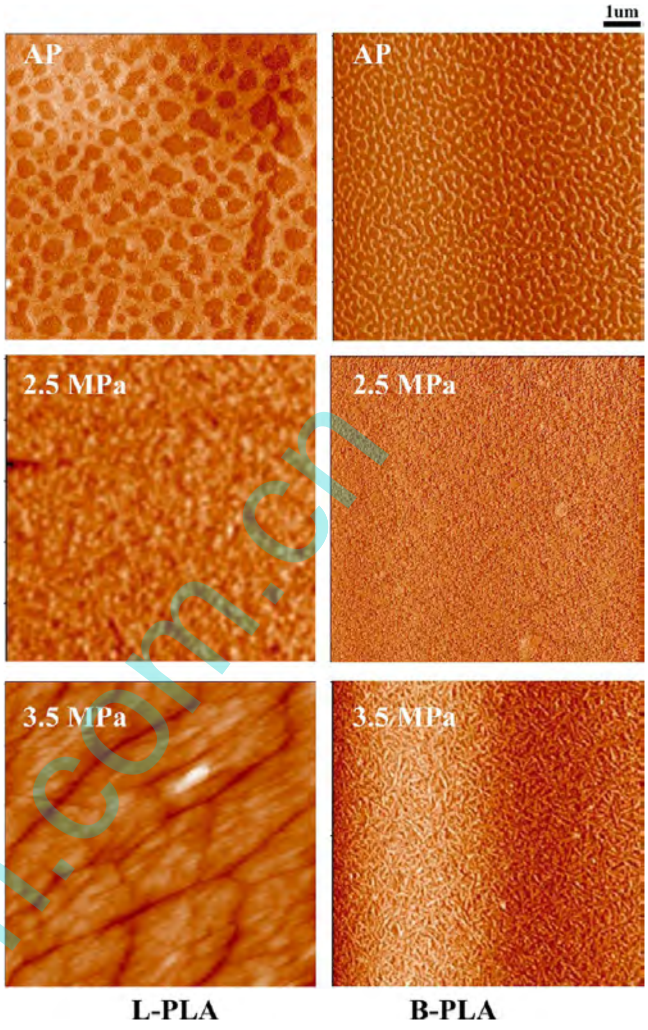

Figure 2. AFM phase images of L-PLA and B-PLA after CO_2 saturation at various conditions.

Foaming Behavior of L-PLA and B-PLA in the Amorphous State. A low CO_2 pressure of 2.5 MPa was applied to saturate PLA specimens, and the treated samples were amorphous before foaming according to DSC measurement. Figure 3 shows the expansion ratio of PLA foams obtained at different foaming temperatures. AL-PLA foam had a high expansion ratio of 21.6 at 70 °C. This value increased to 29.8 at 80 °C. With further increasing the foaming temperature, the expansion ratio of AL-PLA foam decreased significantly to 14.7 at 90 °C and then decreased to 9.2 at 100 °C, 7.9 at 110 °C, and 1.8 at 120 °C, respectively. In the case of the AB-PLA foam, the expansion ratio of AB-PLA foams increased dramatically from 12.7 at 70 °C to 40.6 at 80 °C. The high

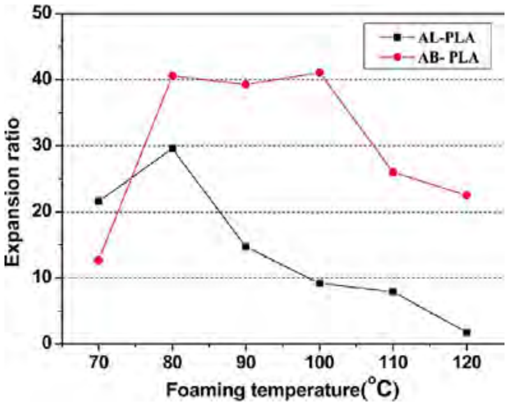

Figure 3. Expansion ratios of AL-PLA and AB-PLA foams obtained at various foaming temperatures. L-PLA and B-PLA resins were amorphous after CO_2 saturation.

expansion ratio of the PLA foam of 40.6 is similar to that of PLA foams obtained by the extrusion foaming.[5,16] The further increase of foaming temperature from 80 to 100 °C did not change the expansion ration of AB-PLA foams. At higher foaming temperature, the expansion ratio of AB-PLA foams decreased to 26.0 at 110 °C and 22.5 at 120 °C. These results demonstrated that AB-PLA foams had a higher expansion ratio and broader optimum foaming windows than AL-PLA foams, when the saturated PLA were amorphous before foaming. Here, the optimum foaming window was noted as the foaming temperature to obtain the highest expansion ratio. It should be pointed out that the optimum foaming window of B-PLA during the solid state foaming was about 20 °C, which is much broader than that of B-PLA foamed by the extrusion foaming, i.e., 6−8 °C.[16]

Figures 4 and 5 show the SEM micrographs of AL-PLA and AB-PLA foams. For AL-PLA foams, the cells with close cell structures and smooth cell walls were observed at the foaming temperatures of 70 and 80 °C. At 90 °C, many wrinkles could be seen in cell walls, suggesting the occurrence of foam shrinkage. At higher foaming temperatures of 100 and 110 °C, the cell opening was found among cell structures because of the cell coalescence. A further increase of the foaming temperature to 120 °C led to a significant decrease in the number of cell structures. For AB-PLA foams, the cell structure could be stable at the foaming temperature up to 100 °C. At 110 and 120 °C, the obvious cell coalescence occurred, resulting in the formation of open cells.

Figure 6 summarizes the cell density of AL-PLA and AB-PLA foams. For AL-PLA foams, they had a similar cell density of 10^6 cells/cm^3 at 70−90 °C. At higher foaming temperatures, however, the cell density decreased dramatically to 3.4×10^5 cells/cm^3 at 100 °C, 5.5×10^4 cells/cm^3 at 110 °C, and 2×10^3 cells/cm^3 at 120 °C, respectively. For AB-PLA foams, they had a cell density of 10^6 cells/cm^3 at 70−100 °C, which was the same with that of AL-PLA foams obtained at 70−90 °C. The increase in foaming temperature decreased the cell density of AB-PLA foams gradually to 8.0×10^5 at 110 °C and 1.7×10^5 cells/cm^3 at 120 °C. At these foaming temperatures, the cell density of AB-PLA foams was about 1−2 order of magnitude higher than that of AL-PLA foams.

Different from the extrusion foaming and injection molding foaming, the sample is in its solid state during the high pressure treatment in solid state foaming process. When the CO_2 saturated specimen is put into the heating medium, it can be foamed once its plasticized T_g is lower than the foaming temperature.[41,42] At low foaming temperatures, the cell growth is governed by the stiffness of polymer matrix.[43] The increased foaming temperature decreases the stiffness of polymer matrix, which leads to the increased expansion ratio with increasing the foaming temperature.[41−43] We believed that the stiffness of polymer matrix was a dominant factor to determine the cell growth and foam expansion of AL-PLA at the foaming temperatures of 70−80 °C. At high foaming temperatures such as 100−120 °C, AL-PLA foams presented the significantly decreased expansion ratio, the decreased cell density as well as the presence of open cell structure, which was caused by cell coalescence. This result demonstrated that the foaming

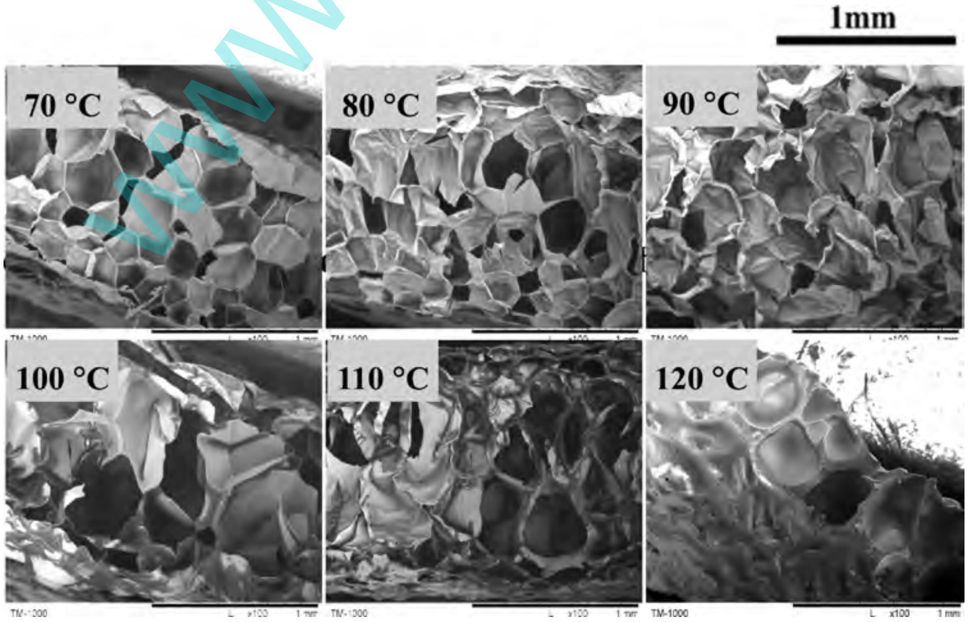

Figure 4. SEM micrographs of AL-PLA foams obtained at various foaming temperatures. L-PLA resin was amorphous after CO_2 saturation.

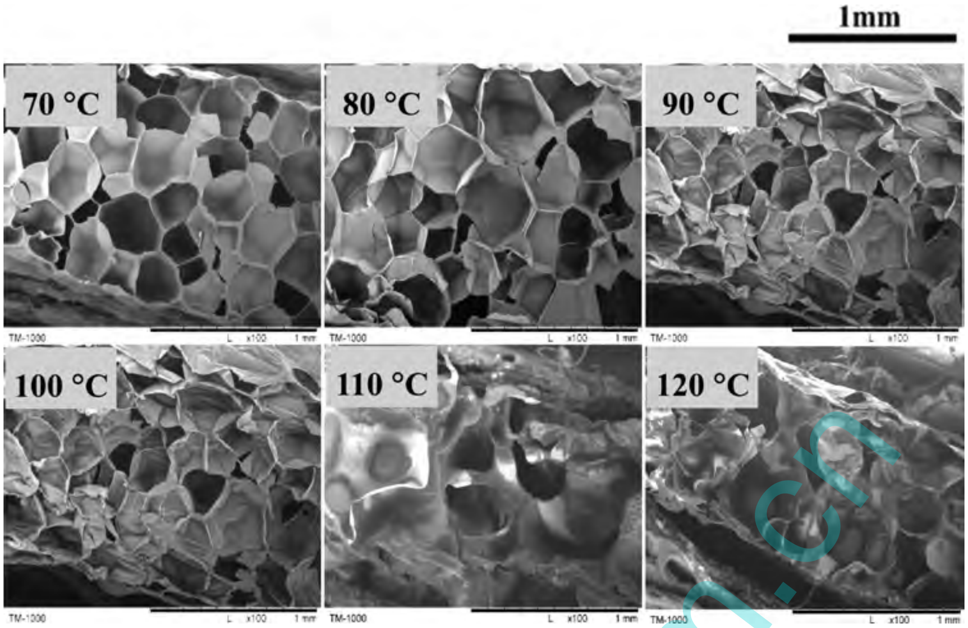

Figure 5. . SEM micrographs of AB-PLA foams obtained at various foaming temperatures. B-PLA resin was amorphous after CO_2 saturation.

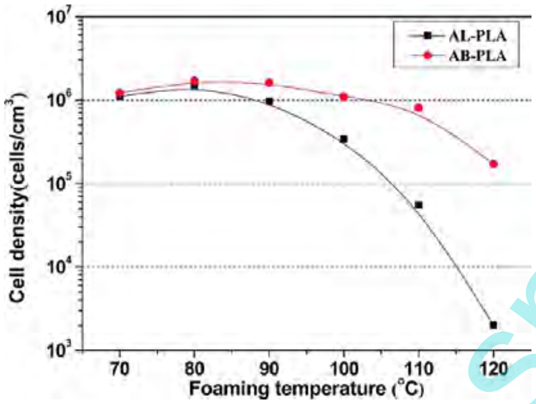

Figure 6. Cell densities of AL-PLA and AB-PLA foams obtained at various foaming temperatures.

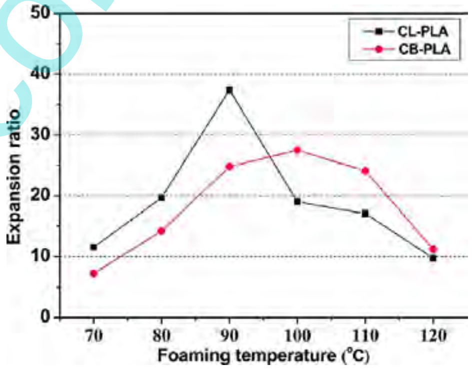

Figure 7. Expansion ratio of CL-PLA and CB-PLA foams obtained at various foaming temperatures. L-PLA and B-PLA resins were crystalline after CO_2 saturation.

temperatures might be higher than the viscous flow temperature of the plasticized L-PLA, and the viscoelastic properties of polymer melt determined the foaming behavior of polymer. The above phenomenon is very common for polymers with low melt strength such as PP, which presents poor foaming behavior during extrusion foaming and batch foaming.[44−46] Compared with AL-PLA foams, however, AB-PLA foams exhibited higher expansion ratio of 22.5−40 vs, 9.2−1.8 at 100−120 °C, a broader optimum foaming temperature window, and a higher cell density of 10^{5-6} vs 10^{3-5} cells/cm^3 at 100−120 °C, which indicated that the improved viscoelastic properties did improve the foaming behavior of AB-PLA.

Foaming Behavior of L-PLA and B-PLA in the Crystalline State. As mentioned above, PLA could be crystallized under CO_2 saturation at the pressure of 3.5 MPa. The effect of crystal domains on the foaming behavior of CL-PLA and CB-PLA were investigated. Figure 7 shows the expansion ratio of PLA foams at various foaming temperatures. For CL-PLA, the foamed samples had an expansion ratio of 11.5 at 70 °C, and the increase of foaming temperature tended to increase the expansion ratio of CL-PLA foams to 19.7 at 80 °C and to 37.4 at 90 °C. At higher foaming temperature, it is found that the expansion ratio of CL-PLA foams decreased significantly to 19.0 at 100 °C and gradually decreased to 17.1 at 110 °C and 9.7 at 120 °C. The expansion ratio of CB-PLA foams exhibited an increased tendency with the foaming temperature at 70−100 °C, and the highest expansion ratio of 27.5 was achieved at 100 °C. A further increase in foaming temperature decreased the cell density slightly to 24.1 at 110 °C and then to 11.2 at 120 °C.

Figures 8 and 9 show the SEM micrographs of CL-PLA and CB-PLA foams at the different foaming temperatures. For CL-PLA foams, the cells with uniform cell distribution, close cell structure, and smooth cell wall could be seen at 70−100 °C. At 110 °C, the cells with wrinkle cell wall were observed, indicated the occurrence of shrinkage after foaming. At 120 °C, the cell opening occurred due to cell coalescence. For CB-PLA, the foamed samples at all foaming conditions exhibited uniform cell distribution and close cell structure, and no obvious cell opening was seen even at the highest foaming temperature of 120 °C.

Figure 10 summarizes the cell density of CL-PLA and CB-PLA foams. CL-PLA foams had a cell density of about 1.5 × 10^7 cells/cm^3 at the foaming temperatures of 70−100 °C. At higher

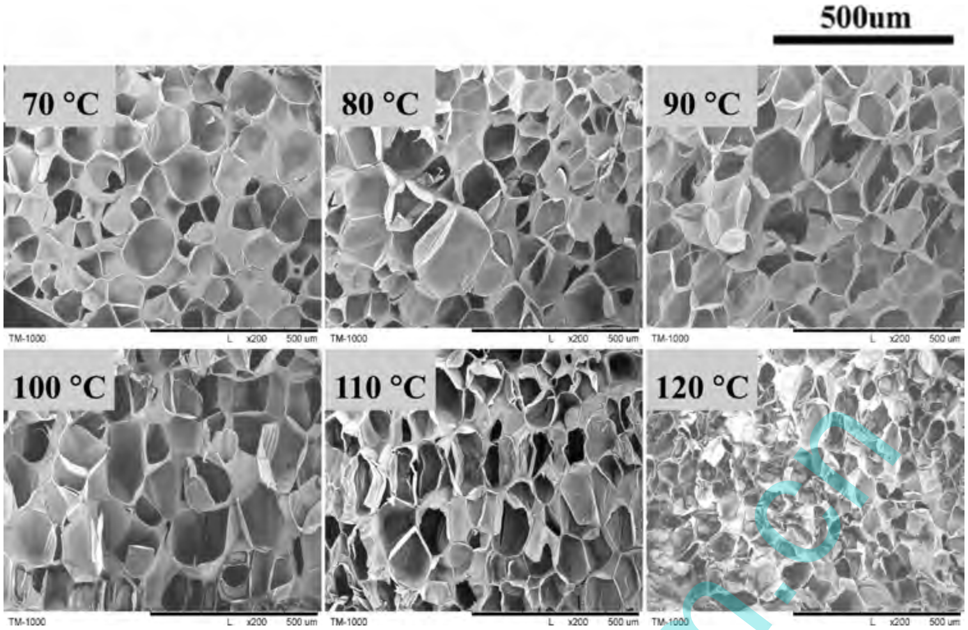

Figure 8. SEM micrographs of CL-PLA foams obtained at various foaming temperatures. L-PLA resin was crystalline after CO_2 saturation.

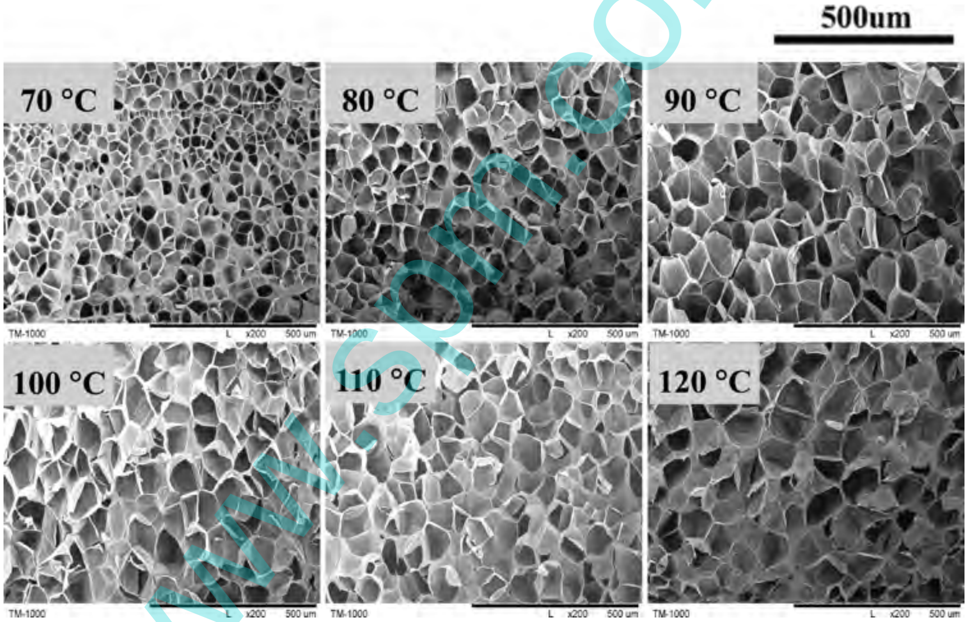

Figure 9. SEM micrographs of CB-PLA foams obtained at various foaming temperatures. B-PLA resin was crystalline after CO_2 saturation.

foaming temperatures, it decreased to 8.8×10^6 cells/cm^3 at 110 °C and then to 3.9×10^6 cells/cm^3 at 120 °C. CB-PLA foams presented a cell density of about 5.9×10^7 cells/cm^3 at 70−100 °C, which was about 4 times higher than that of CL-PLA foams obtained at the same foaming conditions. At higher foaming temperatures, it decreased slightly to 4.5×10^7 cells/cm^3 at 110 °C and 2.6×10^7 cells/cm^3 at 120 °C, which was about 5−7 times higher than that of CL-PLA foams at the foaming conditions. These results demonstrated that CB-PLA foams possessed higher cell density relative to CL-PLA foams at all foaming temperatures.

According to classical nucleation theory, an increase in CO_2 solubility tends to enhance cell nucleation,[47,48] resulting in increased cell density.[42] In this study, it was difficult to explain the significant improvement in foaming behavior of PLA just based on the slightly increased CO_2 pressure from 2.5 to 3.5 MPa. As measured by Wang et al., the CO_2 solubility in PLA only slightly increased from 9.8% to 13.2% at the corresponding CO_2 pressure.[20] We believed that the presence of crystal domains could be the possible mechanism for the improved foaming behavior of PLA, which could make contributions to both the cell nucleation and cell growth processes.

The crystallized domain is often treated as the inert nucleation agent because it cannot absorb the compressed gas. According to the classical heterogeneous nucleation theory,[47,48] the decreased energy barrier for cell nucleation at crystalline/amorphous interfaces facilitates the improvement of cell nucleation,[28] which enhances cell nucleation. By comparing the cell density of L-PLA and B-PLA foams obtained at 2.5 and 3.5 MPa, we observed that the occurrence of crystallization led

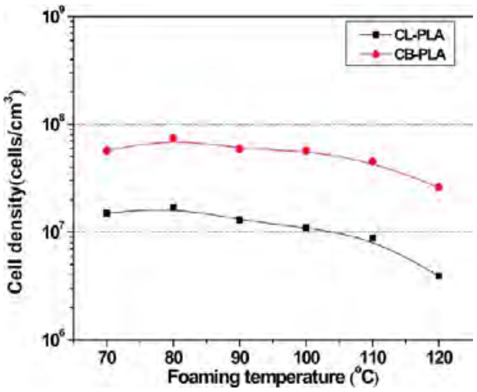

Figure 10. Cell densities of CL-PLA and CB-PLA foams obtained at various foaming temperatures.

to the increase in cell density of about 1 or 2 orders of magnitude for L-PLA foams and of about 1 order of magnitude for B-PLA foams. This phenomenon verified that the induced crystal domains enhanced the cell nucleation behavior during PLA foaming.

As indicated in Figure 6, AL-PLA and AB-PLA foams possessed similar cell densities of 1.5 × 10^6 cells/cm^3 at 70−80 °C, while they increased to 1.5 × 10^7 and 5.9 × 10^7 cells/cm^3, respectively, at 70−90 °C as indicated in Figure 10. Considering no obvious cell coalescence would occur at low foaming temperature, it was suggested that the formed crystal domains during CO_2 saturation might show different effects on cell nucleation behavior. Table 1 indicated that the CO_2 saturated L-PLA and B-PLA at 3.5 MPa possessed the similar crystallinity. Figure 2 further indicated that CB-PLA exhibited a much smaller crystal size than that of CL-PLA. It was speculated that the crystal domains with smaller size supplied more nucleating sites, which enhanced the cell nucleation. A similar phenomenon had been observed in our previous study, PLA/silica nanocomposites possessed smaller crystal size and larger crystal density, and the obtained PLA/silica foam presented the increased cell density in relative to pure PLA foam.[23]

It is well accepted that the occurrence of induced crystallization of the polymer in glass and elastomeric states tends to increase the stiffness of the polymer matrix. As a consequence, the crystallization tended to affect the cell growth and then foam expansion processes at low foaming temperatures of 70−80 °C. When AL-PLA was foamed from its amorphous state, the obtained AL-PLA foams presented the increased expansion ratio from 21.6 at 70 °C to 29.6 at 80 °C. When CL-PLA was foamed from its crystalline state, the obtained CL-PLA foams showed the increased expansion ratio from 11.5 at 70 °C to 19.7 at 80 °C. It is clear that the induced crystallization decreased the expansion ratio of L-PLA foams at the above foaming temperatures. B-PLA foams exhibited the similar phenomenon, where the presence of crystalline domains significantly decreased the foam expansion from 12.7 to 7.2 at 70 °C, from 40.6 to 14.2 at 80 °C. These results might be due to the suppressed cell growth and foam expansion, possibly caused by the increased stiffness of the polymer matrix after crystallization.

At high foaming temperature, where the CO_2 plasticized polymer is in its viscous flow state, the viscoelastic properties becomes the critical parameter to determine the cell growth and foam expansion.[35] The gas saturated L-PLA possessed poor melt viscoelasic properties at the foaming temperature higher than 100 °C. When the CO_2 saturated L-PLA was in its amorphous state, the prepared AL-PLA foams exhibited a decreased cell density from 10^5 to 10^3 cells/cm^3 and the decreased expansion ratio from 9.2 to 1.8 with increasing the foaming temperatures, because of the serious cell coalescence. Once L-PLA was induced crystallization after CO_2 saturation, however, CL-PLA foams only exhibited a slight decrease in cell density from 1.1 × 10^7 to 3.9 × 10^6 cells/cm^3 and the decrease in expansion ratio from 19.0 to 9.7. These interesting results were caused by the improved viscoelastic properties of L-PLA after crystallization. As discussed in the previous studies, the crystal domains could act as physical cross-linking agents, which restricted the relaxation of polymer chains, and thus stabilized the cell structure.[4,5] The induced crystallization presented the obvious different effects on the expansion ratio of B-PLA foams in relative to those of L-PLA foams at the foaming temperatures higher than 100 °C. It is seen that the presence of crystal domains decreased the expansion ratio of B-PLA foams from 41.1 to 27.5 at 100 °C, from 26.0 to 24.1 at 110 °C, and from 22.5 to 11.2 at 120 °C, respectively. These results suggested that the further improved melt viscoelastic properties of CB-PLA hindered the foam expansion. The possible reason was that the melt viscoelastic properties might be too much (in other words, the melt strength might be too high) for CB-PLA for full expansion, when it possessed both the branched chain structure and the crystal domains.

It was interesting to find that the foamed CL-PLA possessed a high expansion ratio of 37.4 at 90 °C, which was much higher than that of the AL-PLA foam obtained at 90 °C, i.e., 14.7. As indicated in Figures 3 and 7, the expansion ratio of PLA foams presented a mountain shape as a function of foaming temperature. This was attributed to the coupling effects of the foaming temperature on the stiffness of the matrix and the viscoelastic properties of the melt. The induced crystallization also presented an obvious influence on the stiffness of the matrix and the viscoelastic properties of the polymer melt. We speculated that the occurrence of crystallization might keep CL-PLA still in its elastomeric state but not in viscous flow state at 90 °C, which facilitated the foam expansion at the increased foaming temperature.

Quantitatively Comparing the Influences of Branched Chain and Crystal Domains on the Cell Coalescence Phenomenon during PLA Foaming. In this study, both the branched chain structure and induced crystallization tended to improve the viscoelastic properties and then increase the foamability of PLA. An interesting question is which factor will be more efficient to improve the foaming behavior of PLA? If induced crystallization is possible, the preparation of the PLA foam by using regular PLA may be more economical because it is much cheaper than high melt strength PLA. Therefore, it is necessary to quantitatively investigate the effects of branched chain and induced crystallization on the foaming behavior of PLA.

During the solid state foaming, the foaming time is a critical parameter to control the cell growth process.[45,49] The extension of foaming time means that the cell structure has an extended time to grow. The effect of the branched chain structure and crystal domains on the cell growth during PLA foaming was investigated by controlling the foaming time. Figure 11 shows the expansion ratio of L-PLA and B-PLA foams obtained at the foaming temperature of 120 °C for 10−60 s. At these foaming conditions, the significant cell coalescence would occur based

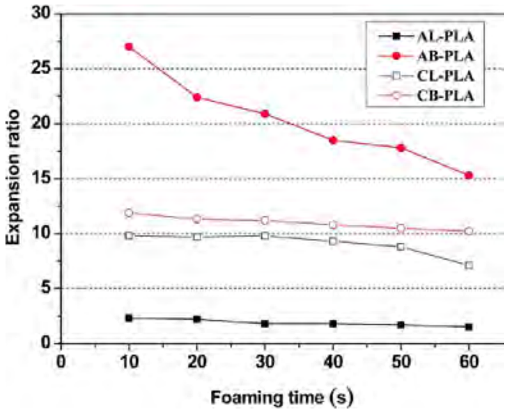

Figure 11. Expansion ratios of AL-PLA, AB-PLA, CL-PLA, and B-PLA foams obtained at the foaming temperature of 120 °C for various foaming times.

on the experimental results mentioned above. For AL-PLA foams, they only had the expansion ratio of 2.2−2.3 for 10−20 s, and the extension of foaming time decreased the values to 1.5−1.8. These results suggested that the nucleated cells tended to coalesce seriously even in the early stage of foaming, caused by the poor viscoelastic properties of AL-PLA. B-PLA, synthesized by chain extending of L-PLA, exhibited the dramatically improved foaming behavior. It is seen that the expansion ratio of the AB-PLA foam was 27.0 for 10 s, and the extension of foaming time decreased the expansion ratio of foams gradually to 22.4 for 20 s, 20.9 for 30s, 18.5 for 40 s, 17.8 for 50 s, and 15.3 for 60 s, respectively. Compared with AL-PLA foams, AB-PLA foams with the improved viscoelastic properties by introducing the branched chain structure exhibited an increased foam expansion of about 10−15 times, resulting from the suppressed cell coalescence phenomenon. The induced crystallization was also beneficial for the improvement of L-PLA foaming behavior. The prepared CL-PLA foams had the expansion ratio of 9.8 for 10 s, and the

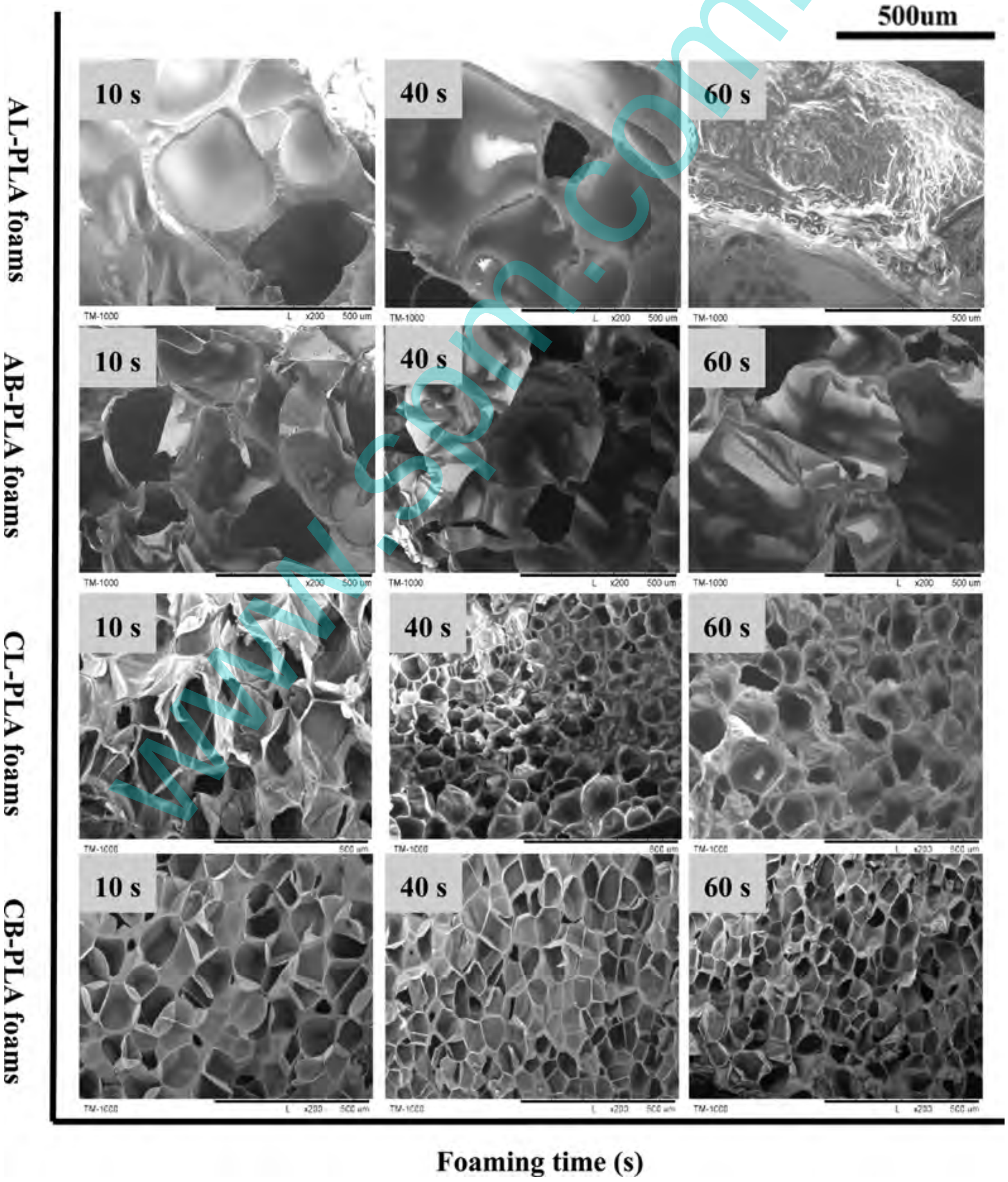

Figure 12. SEM micrographs of AL-PLA, AB-PLA, CL-PLA, and CB-PLA foams prepared at 120 °C for 10, 40, and 60 s, respectively.

extension of foaming time decreased the value to 9.7 for 20 s, 9.8 for 30 s, 9.3 for 40 s, 8.8 for 50 s, and 7.1 for 60 s, respectively. These results suggested that the induced crystallization increased the expansion ratio of CL-PLA foam of about 4 times. Based on the comparison of expansion ratio data of PLA foams, it seems that the introduction of branched chain might be more efficient for the preparation of PLA foam with high expansion ratio in relative to the induced crystallization in this study. Does it mean that the branched PLA possessed higher melt strength than the crystallized PLA and thus suppressed cell coalescence with higher degree? As indicated in Figure 11, actually, the additional crystallization dramatically reduced the expansion ratio of B-PLA foams. This result suggested that the induced crystallization might endow PLA with excessively high melt strength, which restricted the cell growth and foam expansion. Further evidence was that AB-PLA foams exhibited higher dependency with the foaming time compared with CB-PLA foams and AL-PLA foams, which indicated the cell structure exhibited higher thermal stability once the CO_2 saturated PLA crystallized. It should be pointed out that the crystallization of CL-PLA and CB-PLA could be developed continuously during the foaming process,[4−6,25] as indicated in Table 1, because the foaming temperatures was close to the crystallization temperature of the saturated PLA.[50]

Figures 12 and 13 show the SEM micrographs and cell densities of PLA foams prepared at 120 °C for 10−60 s, respectively. AL-PLA foams exhibited the obvious cell coalescence phenomenon even at 10 s. The cell density of AL-PLA foams was in the range of 10^{3-4} cells/cm^3. AB-PLA foams presented large cell size and thin cell wall. As indicated in Figure 13, the cell density of AB-PLA foams decreased obviously from 4.9×10^5 cells/cm^3 at 10 s to 8.0×10^4 cells/cm^3 at 40 s and 3.0×10^4 cells/cm^3 at 60 s. These results suggested that the presence of branched structure improved the viscoelastic properties of PLA, stabilized the cell structure, but it was difficult to suppress the occurrence of cell coalescence phenomenon completely. For CL-PLA foams, they exhibited small cell size and close cell structure at 10 s. The extension of foaming time tended to decrease the cell size at 40 s and increased the cell wall thickness at 60s. Considering the cell density of CL-PLA foams decreased from 4.5×10^6 cells/cm^3 at 10 s to 2.7×10^6 cells/cm^3 at 40 s and 1.1×10^6 cells/cm^3 at 60 s, we speculated that the cell shrinkage and then the following cell coalescence might occur with the extension of foaming time at the foaming temperature of 120 °C. For CB-PLA foams, they possessed uniform cell distribution, close cell structure, and the reduced cell size. These phenomena accompanying the nonchanged cell density of $1.1−2.6 \times 10^7$ cells/cm^3 at 10−60 s indicated that the cell coalescence could be suppressed efficiently by introducing both the branched structure and the crystal domains.

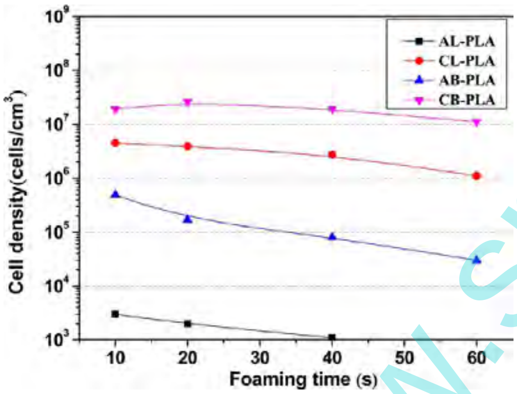

Figure 13. Cell densities of AL-PLA, AB-PLA, CL-PLA, and CB-PLA foams prepared at 120 °C and different foaming times.

In summary, the experimental results verified that the presence of crystal domains enhanced the cell nucleation, increased the stiffness of polymer matrix at lower foaming temperatures and improved the viscoelastic properties of polymer melt at higher foaming temperatures. They contributed to the increased cell density of L-PLA and B-PLA foams and the increased expansion ratio of L-PLA foams at 100−120 °C. More importantly, the induced crystallization endowed L-PLA foam with the highest expansion ratio of 37.4. These results demonstrated that it was possible to get satisfied PLA foams by using the regular PLA resin through the solid state foaming technology.

CONCLUSIONS

In this study, L-PLA and B-PLA with the same D content and similar molecular weight were selected to investigate the influences of long chain branching and induced crystallization on the foaming behavior of PLA during the solid state foaming. Compared with L-PLA, B-PLA with a long chain branching structure possessed the improved viscoelastic properties and the reduced crystal size after induced crystallization by the compressed CO_2. When the saturated PLA samples were in an amorphous state, the prepared AB-PLA foams presented a higher expansion ratio, higher cell density, and broader optimum foaming temperature window relative to AL-PLA foams. When the saturated PLA samples were crystallized, however, CL-PLA and CB-PLA foams exhibited the increased cell density due to the enhanced cell nucleation. Furthermore, CL-PLA foams possessed a higher expansion ratio and higher cell structure stability at the extended foaming times relative to AL-PLA foams. These results demonstrated that it is possible to prepare a well-defined PLA foam by using the regular PLA resin in solid state foaming. For B-PLA, however, the induced crystallization increased the stiffness of the polymer matrix at low foaming temperatures and further improved the viscoelastic properties of the polymer melt at high foaming temperatures, which tended to reduce the expansion ratio of B-PLA foams at all foaming temperatures.

AUTHOR INFORMATION

Corresponding Author

*E-mail: wtzhai@nimte.ac.cn.

Notes

The authors declare no competing financial interest.

ACKNOWLEDGMENTS

The authors gratefully acknowledge the financial support of the National Natural Science Foundation of China (Grant 51003115).

REFERENCES

(1) Gupta, B.; Revagade, N.; Hilborn, J. Poly(lactic acid) Fiber: An Overview. *Prog. Polym. Sci.* **2007**, *32*, 455−82.

(2) Södegård, A.; Stolt, M. Properties of Lactic Acid Based Polymers and Their Correlation with Composition. *Prog. Polym. Sci.* **2002**, *27*, 1123−1163.

(3) Auras, R.; Harte, B.; Selke, S. An Overview of Polylactides as Packaging Materials. *Macromol. Biosci.* **2004**, *4*, 835−864.

(4) Zhai, W. T.; Ko, Y.; Zhu, W. L.; Wong, A.; Park, C. B. A Study of the Crystallization, Melting, and Foaming Behaviors of Poly(lactic acid) in Compressed CO_2. *Int. J. Mol. Sci.* **2009**, *10*, 5381−5397.

(5) Mihai, M.; Huneault, M. A.; Favis, B. D. Crystallinity Development in Cellular Poly(lactic acid) in the Presence of Supercritical Carbon Dioxide. *J. Appl. Polym. Sci.* **2009**, *113*, 2920−2932.

(6) Wang, X. X.; Kumar, V.; Li, W. Development of Crystallization in PLA during Solid-State Foaming Process Using Sub-Critical CO_2. *Cell. Polym.* **2012**, *31*, 1−18.

(7) Liao, X.; Nawaby, A. V.; Whitfield, P.; Day, M.; Champagne, M.; Denault, J. Layered Open Pore Poly(L-lactic acid) Nanomorphology. *Biomacromolecules* **2006**, *7*, 2937−2941.

(8) Mihai, M.; Huneault, M. A.; Favis, B. D.; Li, H. B. Extrusion Foaming of Semi-Crystalline PLA and PLA/Thermoplastic Starch Blends. *Macromol. Biosci.* **2007**, *7*, 907−920.

(9) Reignier, J.; Gendron, R.; Champagne, M. F. Extrusion Foaming of Poly (lactic acid) Blown with CO_2: Toward 100% Green Material. *Cell. Polym.* **2007**, *26*, 83−115.

(10) Huda, M. S.; Drzal, L. T.; Mohanty, A. K.; Mirsa, M. Effect of Fiber Surface-Treatments on the Properties of Laminated Biocomposites from Poly(lactic acid) (PLA) and Kena Fibers. *Compost. Sci. Technol.* **2008**, *68*, 424−432.

(11) Di, Y.; Iannace, S.; Maio, E. D.; Nicolais, L. Reactively Modified Poly(lactic acid): Properties and Foam Processing. *Macromol. Mater. Eng.* **2005**, *290*, 1083−1090.

(12) Mihai, M.; Huneault, M. A.; Favis, B. D. Rheology and Extrusion Foaming of Chain-Branched Poly(lactic acid). *Polym. Eng. Sci.* **2010**, *50*, 629−642.

(13) Pilla, S.; Kim, S. G.; Auer, G. K.; Gong, S.; Park, C. B. Microcellular Extrusion-Foaming of Polylactide with Chain-Extender. *Polym. Eng. Sci.* **2009**, *49*, 1653−1660.

(14) Pilla, S.; Kramschuster, A.; Yang, L. Q.; Lee, J.; Gong, S. Q.; Turng, L. S. Microcellular Injection-Molding of Polylactide with Chain-Extender. *Mater. Sci. Eng. C* **2009**, *29*, 1258−1265.

(15) Lee, S. T.; Leonard, L.; Jun, J. Study of Thermoplastic PLA Foam Extrusion. *J. Cell. Plast.* **2008**, *44*, 293−305.

(16) Wang, J.; Zhu, W.; Zhang, H.; Park, C. B. Continuous Processing of Low-Density, Microcellular Poly(lactic acid) Foams with Controlled Cell Morphology and Crystallinity. *Chem. Eng. Sci.* **2012**, *75*, 390−99.

(17) Corre, Y. M.; Maazouz, A.; Duchet, J.; Reignier, J. Batch Foaming of Chain Extended PLA with Supercritical CO_2: Influence of the Rheological Properties and the Process Parameters on the Cellular Structure. *J. Supercrit. Fluids* **2011**, *58*, 177−188.

(18) Di, Y. S.; Lannace, S.; Di Maio, E.; Nicolais, L. Poly(lactic acid)/Organoclay Nanocomposites: Thermal, Rheological Properties and Foam Processing. *J. Polym. Sci. Part B: Polym. Phys.* **2005**, *43*, 689−698.

(19) Fujimoto, Y.; Ray, S. S.; Okamoto, M.; Ogami, A.; Yamada, K.; Ueda, K. Well-Controlled Biodegradable Nanocomposite Foams: From Microcellular to Nanocellular. *Macromol. Rapid Commun.* **2003**, *24*, 457−461.

(20) Wang, X.; Kumar, V.; Li, W. Low Density Sub-Critical CO_2-Blown Solid-State PLA Foams. *Cell. Polym.* **2007**, *26*, 11−35.

(21) Matuana, L. M. Solid State Microcellular Foamed Poly(lacticacid): Morphology and Property Characterization. *Bioresour. Technol.* **2008**, *99*, 3643−3650.

(22) Matuana, L. M.; Faruk, O. Effect of Gas Saturation Conditions on the Expansion Ratio of Microcellular Poly(lactic acid)/Wood-Flour Composites. *eXPRESS Polym. Lett.* **2010**, *49*, 621−631.

(23) Ji, G. Y.; Zhai, W. T.; Lin, D. P.; Ren, Q.; Zheng, W. G.; Jung, D. W. Microcellular Foaming of Poly(Lactic Acid)/Silica Nanocomposites in Compressed CO_2: Critical Influence of Crystallite Size on Cell Morphology and Foam Expansion. *Ind. Eng. Chem. Res.* **2013**, *52*, 6390−6398.

(24) Ji, G. Y.; Wang, J.; Zhai, W. T.; Lin, D. P.; Zheng, W. G. Tensile Properties of Microcellular Poly(lactic acid) Foams Blown by Compressed CO_2. *J. Cell. Plast.* **2013**, *49*, 101−117.

(25) Wang, J.; Zhai, W. T.; Ling, J. Q.; Shen, B.; Zheng, W. G.; Park, C. B. Ultrasonic Irradiation Enhanced Cell Nucleation in Microcellular Poly(lactic Acid): A Novel Approach to Reduce Cell Size Distribution and Increase Foam Expansion. *Ind. Eng. Chem. Res.* **2011**, *50*, 13840−13847.

(26) Nofar, M.; Zhu, W.; Park, C. B. Effect of Dissolved CO_2 on the Crystallization Behavior of Linear and Branched PLA. *Polymer* **2012**, *53*, 3341−3353.

(27) Lan, Q. F.; Yu, J.; He, J. S.; Maurer, F. H. J.; Zhang, J. Thermal Behavior of Poly(L-lactic) Having Low L-Isomer Content of 94% After Compressed CO_2 Treatment. *Macromolecules* **2010**, *43*, 8602−8609.

(28) Baldwin, D. F.; Park, C. B.; Suh, N. P. A Microcellular Processing Study of Poly(ethylene terephthalate) in the Amorphous and Semicrystalline States. Part I: Microcell Nucleation. *Polym. Eng. Sci.* **1996**, *36*, 1437−1445.

(29) Taki, K.; Kitano, D.; Ohshima, M. Effect of Growing Crystalline Phase on Bubble Nucleation in Poly(L-Lactide)/CO_2 Batch Foaming. *Ind. Eng. Chem. Res.* **2011**, *50*, 3247−3252.

(30) Liao, R.; Yu, W.; Zhou, C. X. Rheological Control in Foaming Polymeric Materials: II. Semi-Crystalline Polymers. *Polymer* **2010**, *51*, 6334−6345.

(31) Xu, M. Z.; Jiang, X. L.; Liu, T.; Hu, G. H.; Zhao, L.; Yuan, W. K. Foaming of Polypropylene with Supercritical Carbon Dioxide. *J. Supercrit. Fluids* **2007**, *41*, 299−310.

(32) Jiang, X. L.; Liu, T.; Xu, Z. M.; Zhao, L.; Hu, G. H.; Yuan, W. K. Effects of Crystal Structure on the Foaming of Isotactic Polypropylene Using Supercritical Carbon Dioxide as a Foaming Agent. *J. Supercrit. Fluids* **2009**, *48*, 167−175.

(33) Lan, X. Q.; Zhai, W. T.; Zheng, W. G. Critical Effects of Polyethylene Addition on the Autoclave Foaming Behavior of Polypropylene and the Melting Behavior of Polypropylene Foams Blown with n-Pentane and CO_2. *Ind. Eng. Chem. Res.* **2013**, *52*, 5655−5665.

(34) Fischer, E. W.; Sterzel, H. J.; Wegner, G. Investigation of the Structure of Solution Grown Crystals of Lactide Copolymers by Means of Chemical Reaction. *Kolloid-Zu Z-Polymer* **1973**, *251*, 980−990.

(35) Stange, J.; Münstedt, H. Rheological Properties and Foaming Behavior of Polypropylenes with Different Molecular Structures. *J. Rheol.* **2006**, *50*, 907−920.

(36) Lips, P. A. M.; Velthoen, I. W.; Dijkstra, P. J.; Wessling, M.; Feijen, J. Gas Foaming of Segmented Poly(ester amide) Films. *Polymer* **2005**, *46*, 9396−9403.

(37) Mizumoto, T.; Sugimura, N.; Moritani, M.; Sato, Y.; Masuoka, H. CO_2-Induced Stereocomplex Formation of Stereoregular Poly(methyl methacrylate) and Microcellular Foams. *Macromolecules* **2000**, *33*, 6757−6763.

(38) Zhai, W. T.; Yu, J.; Ma, W. M.; He, J. S. Influence of Long-Chain Branching on the Crystallization and Melting Behavior of Polycarbonates in Supercritical CO_2. *Macromolecules* **2007**, *40*, 73−80.

(39) Marubayashi, H.; Akaishi, S.; Akasaka, S.; Asai, S.; Sumita, M. Crystalline Structure and Morphology of Poly(L-Lactide) Formed under High-Pressure CO_2. *Macromolecules* **2008**, *41*, 9192−9203.

(40) Takada, M.; Hasegawa, S.; Ohshima, M. Crystallization Kinetics of Poly(L-lactide) in Contact with Pressurized CO_2. *Polym. Eng. Sci.* **2004**, *44*, 186−196.

(41) Krause, B.; Mettinkhof, R.; van der Vegt, N. F. A.; Wessling, M. Microcellular Foaming of Amorphous High-T_g Polymers Using Carbon Dioxide. *Macromolecules* **2001**, *34*, 874−884.

(42) Arora, K. A.; Lesser, A. J.; McCarthy, T. J. Preparation and Characterization of Microcellular Polystyrene Foams Processed in Supercritical Carbon Dioxide. *Macromolecules* **1998**, *31*, 4614−4620.

(43) Kumar, V.; Weller, J. Production of Microcellular Polycarbonate Using Carbon Dioxide for Bubble Nucleation. *J. Eng. Ind.* **1994**, *116*, 413−420.

(44) Zhai, W. T.; Wang, H. Y.; Yu, J.; Dong, J. Y.; He, J. S. Foaming Behavior of Isotactic Polypropylene in Supercritical CO_2 Influenced by Phase Morphology via Chain Grafting. *Polymer* **2008**, *49*, 3146−3156.

(45) Zhai, W. T.; Wang, H. Y.; Yu, J.; Dong, J. Y.; He, J. S. Cell Coalescence Suppressed by Crosslinking Structure in Polypropylene Microcellular Foaming. *Polym. Eng. Sci.* **2008**, *48*, 1312−1321.

(46) Zhai, W. T.; Kuboki, T.; Wang, L.; Park, C. B. Cell Structure Evolution and the Crystallization Behavior of Polypropylene/Clay Nanocomposites Foam Blown in Continuous Extrusion. *Ind. Eng. Chem. Res.* **2010**, *49*, 9834−9845.

(47) Colton, J. S.; Suh, N. P. The Nucleation of Microcellular Thermoplastic Foam with Additives: Part I: Theoretical Considerations. *Polym. Eng. Sci.* **1987**, *27*, 485−492.

(48) Colton, J. S.; Suh, N. P. The Nucleation of Microcellular Thermoplastic Foam with Additives: Part I: Part II: Experimental Results and Discussion. *Polym. Eng. Sci.* **1987**, *27*, 493−499.

(49) Zhai, W. T.; Wang, J.; Chen, N.; Naguib, H. E.; Park, C. B. The Orientation of Carbon Nanotubes in Poly(ethylene-co-octene) Microcellular Foaming and Its Suppression Effect on Cell Coalescence. *Polym. Eng. Sci.* **2012**, *10*, 2078−2089.

(50) Yu, L.; Liu, H.; Dean, K. Thermal Behavior of Poly(lactic acid) in Contact with Compressed Carbon Dioxide. *Polym. Int.* **2009**, *58*, 368−372.